Supplementary information

Triggered Interactions between Nanoparticles and Lipid Membranes: Design Principles for Gel Formation or Disruption-and-Release

Rui Cao[†], *Jingjing Gao*[†], *S. Thayumanavan*[*], *and Anthony D. Dinsmore* [*]
([†]Dr. R. Cao, Dr. J. Gao contributed equally to this work)
Dr. R. Cao, Prof. A.D. Dinsmore, *Department of Physics*
Dr. J. Gao, Prof. S. Thayumanavan, *Department of Chemistry*
University of Massachusetts Amherst, 01003, USA

E-mail: dinsmore@umass.edu, thai@chem.umass.edu

This supplementary section provides Materials and methods; NMR spectra of P0, P1 and P2; dark-field images of bound nanoparticles; absorption spectra; particle sizes by DLS and TEM images; and details of the theoretical prediction for the adhesion-to-destruction crossover.

Materials and Methods:

Materials: The lipids 1,2-dioleoyl-sn-glycero-3-phosphocholine (DOPC) and 1,2-dioleoyl-sn-glycero-3-phospho-(1'-rac-glycerol) (DOPG) were purchased from Avanti Polar Lipid (Alabaster, Alabama, USA). All other reagents were purchased from Millipore-Sigma and used without further purification unless specified otherwise. Azobisisobutyronitrile (AIBN) was recrystallized in ethanol prior to use.

Methods: ^{1}H NMR and ^{13}C NMR spectra were recorded on a Bruker DPX-400 MHz NMR spectrometer using the residual proton resonance of the solvent as the internal standard. Spectra are presented below. The molecular weight of the polymers was measured by gel permeation chromatography (GPC, Agilent) using a PMMA standard with a refractive index detector. THF was used as eluent with a flow rate of 1 mL/min.

P1, P2 nanoparticles preparation: The polymers **P0**, **P1**, and **P2** were synthesized as described procedures listed below. Self-assembled nanoparticles were made with the following procedure: 1 mL 180 mOsm/L glucose aqueous solution was added dropwise to a 100 μL solution of polymer (**P0**, **P1** or **P2**) in acetone (5 mg/mL) and stirred overnight to allow acetone to evaporate. The size and zeta potential of the resulting self-assembled particles were recorded by a Malvern Nanozetasizer ZS90 with a 637-nm laser source with non-invasive backscattering technology detected at 173° using disposable sizing cuvette. Sample was measured at a concentration of 0.2 mg/mL. We refer to nanoparticles composed of **P0**, **P1** and **P2** as **NP0**, **NP1** and **NP2**, respectively.

Transmission Electron Microscopy (TEM): The **NP0**, **NP1** and **NP2** samples were dropped onto carbon-coated copper grid, dried by slow evaporation in air, and then dried in a vacuum overnight. Images were recorded on a JEOL-2000FX electron microscopy operated at 200 kV and at a nominal magnification of 5000×.

Vesicle preparation: Vesicles were made with sucrose inside and a glucose-sucrose mixture outside. In all cases, the osmolarities of the interior and exterior were measured (Vapro model 5600 osmometer) and kept at 180 mOsm/L to avoid osmotic stress. Osmolarity measurements were repeated 3 times and the standard deviation was usually 3-4 mOsm/L. Vesicles were made by

electroformation in a method adapted from prior work[1]: 10mg/mL DOPG and DOPC lipid stock solutions in chloroform were prepared, and the two stock solutions were mixed to achieve a DOPG molar percentage ranging from 0 to 100%. Two clean ITO-coated glass slides were coated, each with 50 μL of the mixed lipid solution and dried under vacuum for 2 h. The ITO slides were held by Teflon spaces with their ITO-coated surfaces facing one another. The gap between them was filled with 3 mL of 180 mOsm/L sucrose solution. Electroformation was carried out at 40 °C with a sinusoidal applied voltage at 10 Hz and peak-to-peak voltage 2.4 V for 105 min. After transferring the vesicle suspension to a vial, we added 2.5 mL of glucose solution of the same osmolarity, allowed the sample to sediment for 24 h, and collected 50 μL of concentrated vesicle suspension.

Microscopy: The dynamics and steady-state response of mixtures of self-assembled particles and vesicles were imaged using optical microscopy. Bright-field images were acquired through two combinations: one is using a Flir blackfly S CMOS camera and a Zeiss 20× Plan Neofluar objective with 0.4 NA, the other one is CoolSnap HQ2 camera (Roper Scientific) and a Zeiss 63× Plan Neofluar objective with 1.4 NA. Dark-field images were acquired using the CoolSnap HQ2 camera and a Zeiss 100× Plan Neofluar objective with 1.3 NA. The CoolSnap camera measures pixel values that are proportional to the light intensity.

Polymer synthesis: Synthesis of molecule **P0**: Monomer **hexanyl coumarinyl mathacrylate (HCM)** and polyethyleneglycol chain transfer reagent (PEG-CTA) were prepared according to previously reported procedures.[2-3] A solution of **HCM** (103 mg, 0.3 mmol), PEG-CTA (150 mg, 0.03 mmol) and AIBN (0.984 mg, 0.006 mmol), in tetrahydrofuran (THF) (400 μL) was degassed by three freeze-pump-thaw cycles before being sealed off under argon protection and vaccum. After 6 h at 65 °C, the polymerization media was diluted in dichloromethane and condensed using a rotavap, and precipitated in diethyl ether for 3 times to remove unreacted monomers. The precipitate was collected and dried under vacuum to yield 233 mg (93% yield) of **P0**. GPC (THF): Mn= 8.8 K Da, Đ= 1.02. ^{1}H NMR (400 MHz, $CDCl_3$) δ 7.45, 6.80, 6.79, 6.07, 3.97, 3.83, 3.66, 3.48, 2.36, 1.96, 1.82, 1.67, 1.50, 1.46, 1.26, 1.06, 0.89. From ^{1}H NMR, integration of peak at δ 6.07 and δ 3.83 provided the molar ratio of PEG/Coumarin to be 1:10. ^{13}C NMR (126 MHz, $CDCl_3$) δ 161.06, 154.19, 151.62, 124.54, 112.39, 111.52, 110.77, 100.16, 76.26, 76.01, 75.75, 69.56, 67.33, 52.41, 28.68, 27.94, 27.42, 27.08, 24.94, 24.74, 17.63.

Synthesis of polymer **P1**: **P0** was dissolved in DCM/TFA (1mL/1mL) mixture and stirred overnight at room temperature. The solvent was evaporated and redissolved in DCM, the solution was then dialyzed against DCM/MeOH to get purified **P1** (95% yield). GPC (THF): Mn= 8.2 K Da, Đ= 1.05. ^{1}H NMR (400 MHz, $CDCl_3$) δ 7.43, 6.78, 6.67, 6.05, 3.95, 3.81, 3.63, 3.45, 2.34, 1.97, 1.80, 1.66, 1.43, 1.24, 1.04, 0.87. ^{13}C NMR (126 MHz, $CDCl_3$) δ 161.13, 160.76, 154.06, 152.17, 124.58, 112.39, 111.72, 110.55, 100.16, 69.35, 69.32, 69.23, 68.88, 67.37, 38.92, 28.68, 27.93, 27.08, 24.94, 24.73, 17.65.

Synthesis of polymer **P2:** 2-nitrobenzyl alcohol (10 eq. per NH_2 of **P1**) was dissolved in dried THF and stir with argon protection at room temperature, triphosgene (15 wt% in toluene, 20 eq. per NH_2 of **P1**) was added to the mixture and stirred for 2 hours, then the solution was rotavaped to remove solvent and dried with vaccum pump for 3 hours to remove extra phosgene. The residue was redissoved in DCM and added to a solution of P1 (100 mg) and triethylamine (10 eq. per NH_2 of **P1**), the solution was stired at room temperature for 8 hours and then dialyzed against DCM/MeOH to get purified **P2** (95% yield). GPC (THF): Mn= 8.2 K Da, Đ= 1.05. ^{1}H NMR (400 MHz, $CDCl_3$) δ 8.07, 7.62, 7.43, 7.26, 6.79, 6.68, 6.06, 5.51, 4.97, 3.96, 3.81, 3.63, 3.47, 3.45,2.36, 1.97, 1.80, 1.66, 1.45, 1.24, 1.05, 0.87. ^{13}C NMR (101 MHz, $CDCl_3$) δ 166.30, 162.06, 161.18,

155.19, 152.64, 145.96, 137.71, 128.35, 127.82, 126.64, 125.55, 113.40, 112.53, 111.77, 101.17, 77.37, 77.05, 76.73, 70.56, 69.65, 68.36, 64.97, 45.61, 45.09, 44.68, 39.98, 29.70, 28.97, 28.11, 25.97, 25.76, 18.65.

Scheme S1. Synthesis route for polymer **P0**, **P1**, and **P2**.

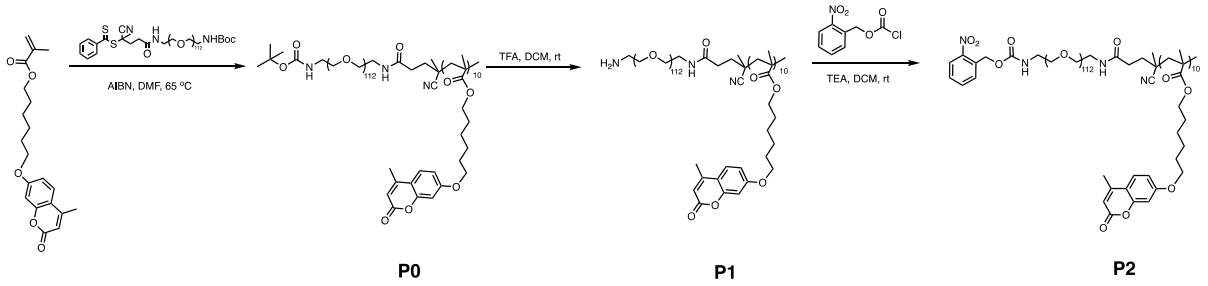

Scheme S2. UV induced photocrosslinking and cleavage of nitrobenzyl group.

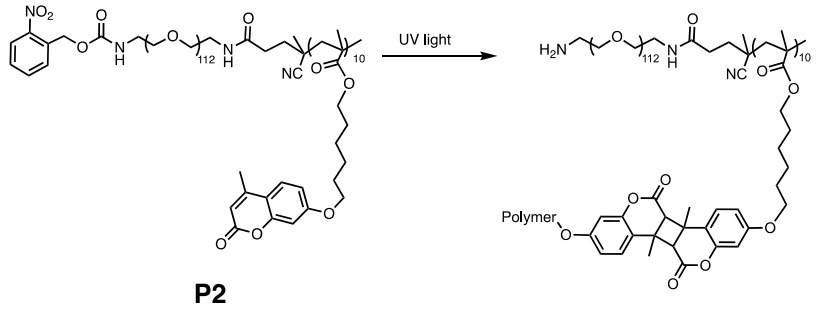

NMR spectra of polymers

NMR of P0

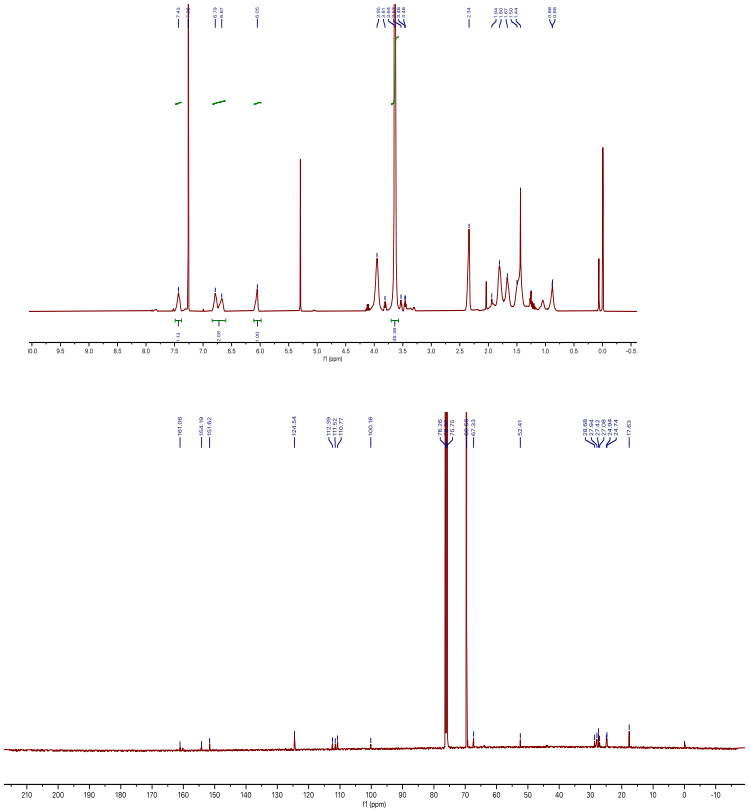

NMR of P1

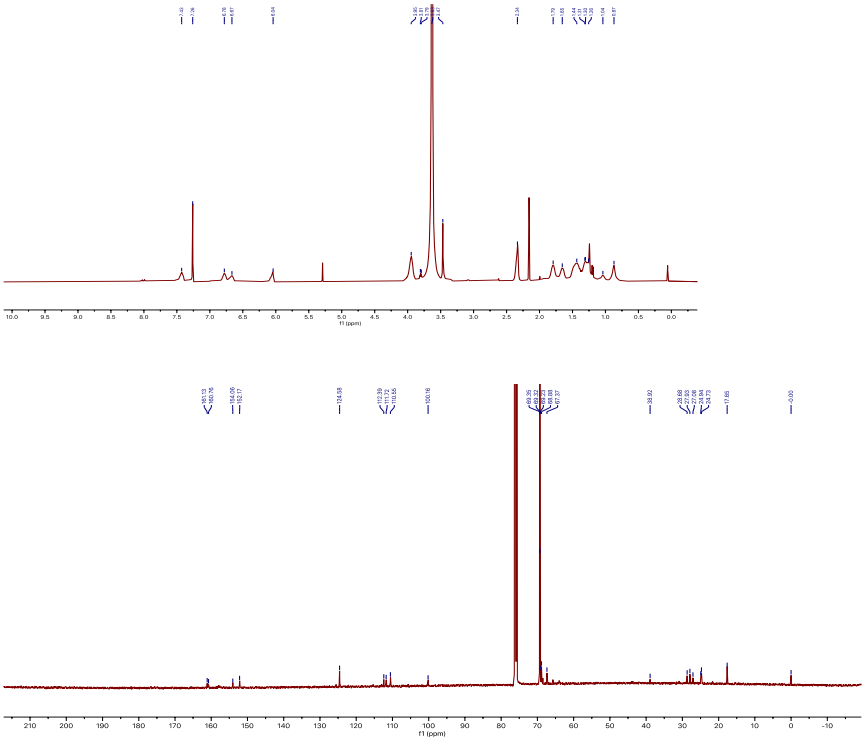

NMR of P2

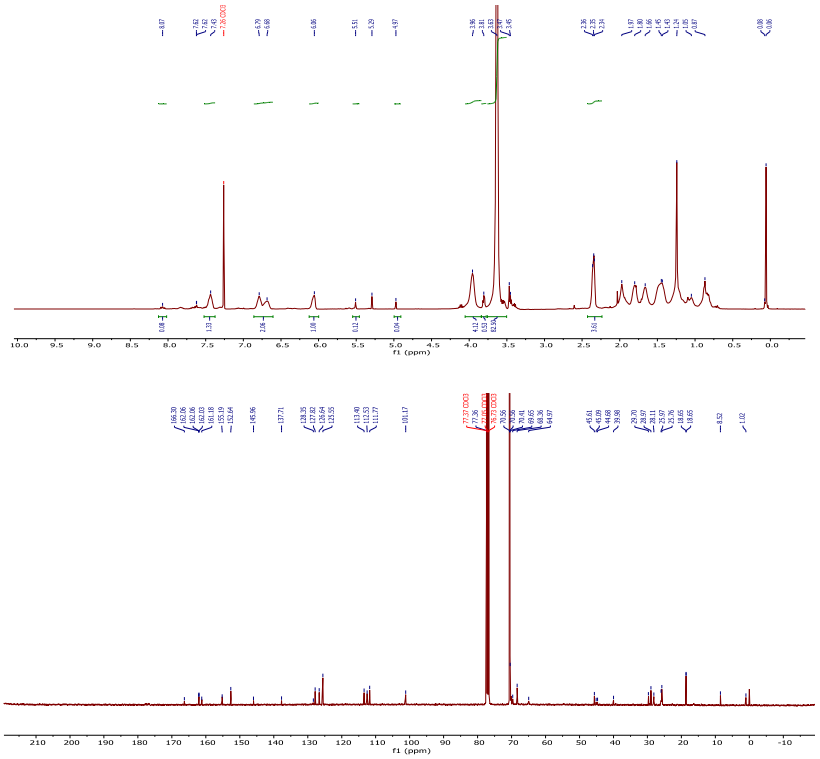

Dark-field optical microscopy of bound nanoparticles:

Dark-field microscopy showed that nanoparticles bound to the membrane. In dark-field imaging, the camera detects light that is scattered by objects in the focal volume. Because the particles are much larger than the membrane thickness (approx. 4 nm), they scatter far more than does the membrane. Figure S1(a) shows a dark-field image of a typical DOPC vesicle ($p_{DOPG} = 0$), showing weak contrast between the membrane and background. We then added 5 μL of **NP1** particle suspension (p_{amine}=100%) to 20 μL of vesicle suspension. After 30 min, the intensity near the membrane was significantly higher, and was higher still in regions where two vesicles adhered to one another (Fig. S1(b)). To quantify the response, we measured the image intensity across a line, divided by the average background intensity. Figure S1(c) shows the normalized intensity measured along the white lines labeled 1, 2 and 3. The plot shows a significant peak located at the membrane, indicating bound particles. The inset shows the peak values at the membrane, averaged over a wider set of repeated measurements. We found peak relative intensitioes equal to 1.043 ± 0.006, 1.37 ± 0.06, and 1.59 ± 0.1 for configurations #1, 2 and 3. Because the particles are small compared to the wavelength of visible light (and hence weakly scattering), we assume that the measured intensity is proportional to the local particle concentration. Hence, the relative bound concentrations in adhered region (#3) relative to the single membrane (#2) was (1.59-1.043)/(1.37-1.043) = 1.7 ± 0.2. From this, we estimate that nanoparticles accumulated in the adhered-membrane region (#3) with a concentation that was 1.7 ± 0.2 times greater than at the exposed membrane (#2).

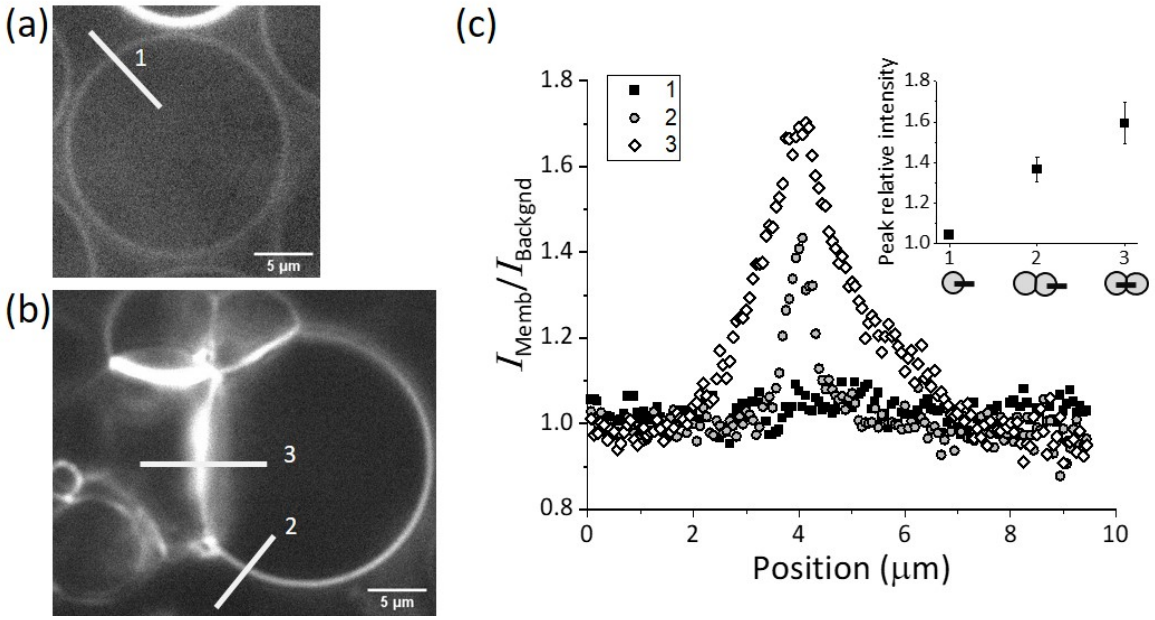

Figure S1. Dark-field images of vesicles and bound nanoparticles. (**a**) DOPC vesicles ($p_{DOPG} = 0$) without particles. (**b**) In the presence of **NP1** particles (p_{amine}= 100%), images show much higher intensity near the membrane. Note that the grayscales of (a,b) are different. (**c**) Plot of relative image intensity along the three line segments shown in white in (**a**,**b**). **Inset**: the mean and standard error of peak relative intensity for a population of at least 14 vesicles in each of the 3 cases: just vesicles (#1); particles and vesicles (#2), and particles and vesicles in regions of vesicle-vesicle adhesion (#3).

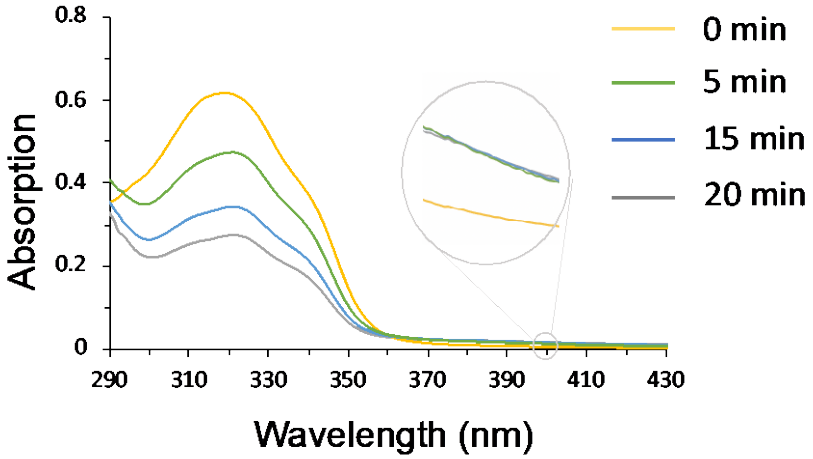

Figure S2. UV irradiation induced nitrobenzyl cleavage in **P2** indicated by absorbance increase at 400 nm and coumarin dimerization indicated by absorbance decrease at 320 nm.

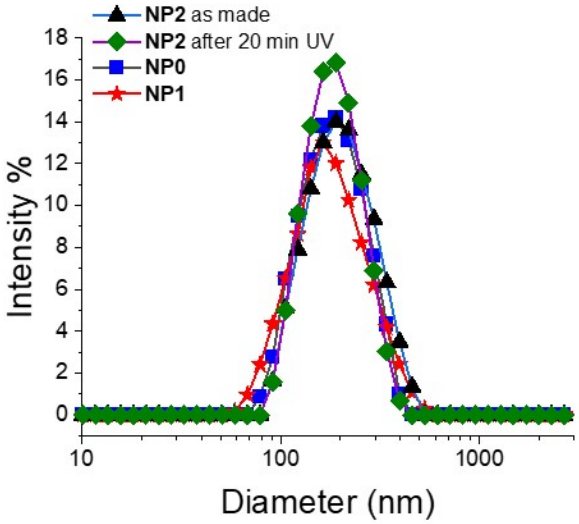

Figure S3. Nanoparticle sizes measured by dynamic light scattering (DLS). From this data we extracted mean diameters of 192 ± 68 nm and 192 ± 83 nm **NP0** and **NP1** respectively. For **NP2**, the diameters were 212 ± 80 nm and 192 ± 61 nm before and after UV exposure. These diameters were indistinguishable within error.

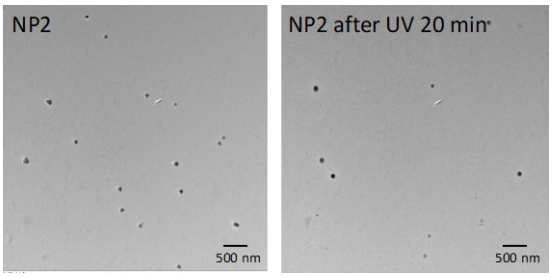

Figure S4. TEM images showed nanoparticles **NP2** had the same morphology before and after UV irradiation.

Prediction of the transition from adhesion to wrapping and destruction

Here we compute the location of the transition from weak adhesion to particle-wrapping and vesicle destruction (Fig. 5b of the main text). We used the Debye-Hückel model to model the electrostatic double-layer interaction.[4] The parameter w was defined as the attractive double-layer interaction energy per area of contact between particle and membrane. (Here, $w > 0$ corresponds to adhesion.) As discussed in the main text, we used the wrapping threshold from previous simulations, showing that

$$\frac{wa^2}{\kappa} = \frac{1}{2}$$

at the transition.[2] This previous result assumed that the range of adhesion was short compared to the particle size. Here, the range of adhesion is set by the Debye screening length l_{D}, which is defined as

$$l_{\mathrm{D}} = \sqrt{\varepsilon\varepsilon_0 k_{\mathrm{B}}T/(2e^2c_0)}\,,$$

where ε and $\varepsilon_0$are the dielectric constant of water and the free-space permittivity, respectively, $k_{\mathrm{B}}T$ is Boltzmann's constant times the temperature in Kelvins, e is the fundamental charge, and c_0 is the concentration of ions (assumed monovalent). In our experiments, we estimated that l_{D} was roughly 15 nm (set by ions leaching in from the glass and air), but in fact the numerical results change little even if l_{D} is 50 nm.

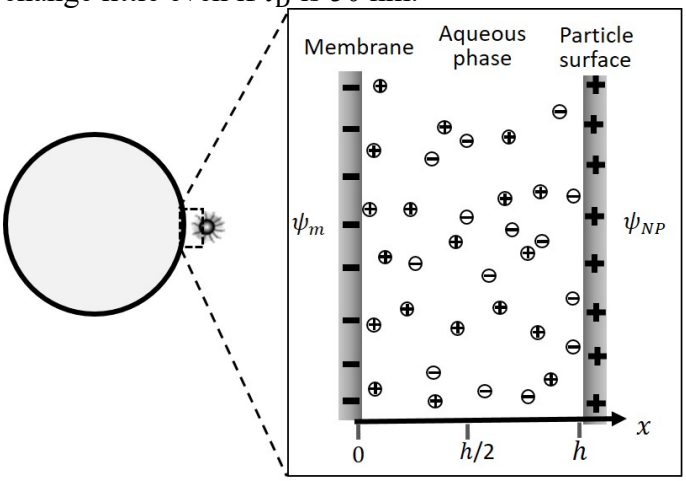

Figure S5: Illustration of the geometry in our model. Because the separation (h) between the membrane and particle is small compared to the particle radius, we can take the two surfaces to be flat at small scales. The parameters ψ_{m} and ψ_{NP} are the electrostatic potentials of the two surfaces.

Because the attracting particle and membrane surfaces will approach much closer than l_{D} (and hence much closer than the particle radius), we can treat both surfaces as flat plates. See Fig. S5. The adhesion free energy per area w between the two plates can be estimated as

$$w = (2\varepsilon\varepsilon_0/l_{\mathrm{D}})\,\psi_p\psi_m \exp(-h/l_{\mathrm{D}}),$$

where ψ_m and ψ_p are the surface potentials on the membrane and particle (here taken to be zeta potentials). Although the surface potentials are in some cases high enough to violate the Debye-Hückel approximation that $e\psi/(k_{\mathrm{B}}T) \ll 1$, this expression works if we use the effective potentials (which is called charge renormalization), which is what one obtains from electrophoretic measurements. When the two surfaces are close to one another, there may also be a shift of the

surface potential owing to charge regulation. The above expression is a compromise between the constant-ψ and constant-charge approximations.

The expressions can be put in convenient dimensionless terms:

$$\frac{w}{k_{\mathrm{B}}T} = \frac{1}{2\pi l_{\mathrm{D}} l_{\mathrm{B}}} \frac{e\psi_p}{k_{\mathrm{B}}T} \frac{e\psi_m}{k_{\mathrm{B}}T}$$

where we have explicitly set $\exp(h/l_{\mathrm{D}}) = 1$ and l_{B} is the Bjerrum length,

$$l_{\mathrm{B}} = \frac{e^2}{4\pi\varepsilon\varepsilon_0 k_{\mathrm{B}}T},$$

which is 7Å in water.

We assumed that both ψ_p and ψ_m increased linearly with p_{Amine} and p_{DOPG}. We used our measured particle zeta potentials for the limiting cases of 0% and 100% amine. For the membrane, we used the literature values for 0% and 100% DOPG.[5] This analysis yielded

$$\psi_p = \frac{k_B T}{e}(-0.31 + 0.83 p_{amine})$$

$$\psi_m = \frac{k_B T}{e}(-0.20 - 3.0 p_{DOPG}),$$

and the numerical values have uncertainties because of the measurement uncertainties in zeta potentials described in the article.

We wrote a Python code to plot the set of (p_{amine}, p_{DOPG}) points that correspond to $\frac{wa^2}{\kappa} = \frac{1}{2}$. We varied the coefficients in the above expressions for $\psi_{p,m}$ within the experimental error bars. The gray region in Fig. 5(b) of the main text encompasses all of the curves that fell in this range.

References:

1. Zuraw-Weston S, W. D., Torres IK, Lee Y, Wang LS, Jiang Z, Lázaro GR, Wang S, Rodal AA, Hagan MF, Rotello VM, Dinsmore AD. Nanoparticles Binding to Lipid Membranes: From Vesicle-Based Gels to Vesicle Tubulation and Destruction. *Nanoscale* **2019**, *10*, 18464-18474.
2. J. Gao, P. Wu, A. Fernandez, J. Zhuang, S. Thayumanavan, *Angew. Chemie - Int. Ed.* **2020**, *59*, 10456-10460.
3. J. Gao, K. Dutta, J. Zhuang, S. Thayumanavan, *Angew. Chem. Int. Ed.* **2020**, *59*, 23466-23470.
4. Russel, W. B., Saville, D. A. & Schowalter, W. *Colloidal Dispersions*. (Cambridge U. Press, 1989).
5. Maity, P., Saha, B., Kumar, G. S. & Karmakar, S. Binding of Monovalent Alkali Metal Ions with Negatively Charged Phospholipid Membranes. *Biochim. Biophys. Acta-Biomembr.* **2016**, *1858*, 706-714.